*Int. J. Heat Mass Transfer.* Vol. 29, No. 5, pp. 769–775, 1986
Printed in Great Britain

0017-9310/86 $3.00 + 0.00
Pergamon Journals Ltd.

# Conjugated, mixed convection–conduction heat transfer along a cylindrical fin in a porous medium

JIN-YUAN LIU,† W. J. MINKOWYCZ† and P. CHENG‡

† University of Illinois at Chicago, Department of Mechanical Engineering, Chicago, IL 60680, U.S.A.
‡ University of Hawaii, Department of Mechanical Engineering, Honolulu, HI 96822, U.S.A.

(*Received* 24 *October* 1985 *and in final form* 26 *December* 1985)

**Abstract**—The problem of mixed convection flow about a vertical, cylindrical fin embedded in a porous medium is studied analytically based on the conjugate convection–conduction theory. A local nonsimilarity solution, up to the third level of truncation, is obtained for the convective flow in the porous medium. The resulting set of ordinary differential equations are coupled with the one-dimensional heat conduction equation in the fin through interfacial conditions. The effects of the conjugate convection–conduction parameter, surface curvature and the mixed convection parameter on the fin temperature distribution, local heat transfer coefficient, local heat flux, total heat transfer and fin efficiency are illustrated. The results of the present analysis are found to have trends similar to those of the classical fluids.

## INTRODUCTION

DURING the past few years, the problems of conjugate heat transfer from a fin have received much attention [1–5]. Results of these analyses have shown that the local heat transfer coefficient varies along the fin. This is in direct contrast with the conventional assumption that the local heat transfer coefficient is constant along a fin. The variations of the heat transfer coefficient are due to the interaction between the fin and its adjacent boundary-layer flow. Thus, in the analysis of heat transfer from a long fin, it is more realistic to leave the heat transfer coefficient unspecified and to treat it as part of the solution.

In a recent paper [6], the problem of conjugate, mixed convection heat transfer from a vertical plate fin embedded in a porous medium was analyzed by Liu *et al.* Results were found to be similar to those of the classical fluids [3]. In particular, for a high convection–conduction parameter, the local heat transfer coefficient was found to decrease at first, attain a minimum, and then increase in the streamwise direction. In the present investigation, attention is given to the analysis of mixed convection flow over a vertical, cylindrical fin embedded in a porous medium with fin–fluid interactions taken into consideration. Since the heat transfer coefficient along the fin is not prescribed *a priori*, it is necessary to solve the heat conduction problem in the fin and the boundary-layer flow adjacent to the fin simultaneously. Because the mixed convective flow in the porous medium does not have a similarity solution, a solution based on the local nonsimilarity model is applied. The resulting set of ordinary differential equations for the boundary-layer flow are coupled with the heat conduction equation through the interfacial conditions. The entire set of equations were solved numerically by iteration [6–8]. Computations were carried out for fin temperature distribution, the local heat transfer coefficient, the local heat flux, the total heat transfer rate and the fin efficiency at different values of the controlling parameters.

## ANALYSIS

Consider a vertical cylindrical fin of radius $r_0$ and length $L$, which is embedded in an isotropic, porous medium at an ambient temperature of $T_\infty$. The base of the fin is attached to a planar wall at $T_b$ which is higher than $T_\infty$. A schematic diagram of the cylindrical fin is presented in Fig. 1 where the origin of the cylindrical coordinate is placed on the tip of the fin, with $x$ and $r$ denoting the vertical (axial) and radial coordinates. The coordinate system is oriented such that the gravitational force acts in the negative $x$-direction. At free stream, a uniform flow with $u_\infty$ is flowing in the positive $x$-direction (i.e. vertically upward). Thus, the buoyancy

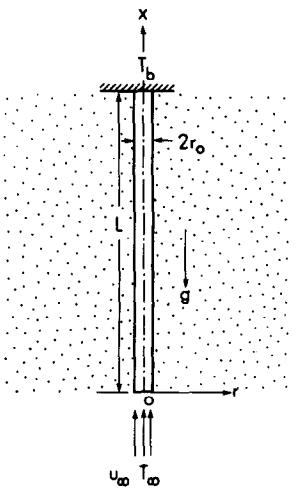


FIG. 1. Schematic diagram of the physical problem.

## NOMENCLATURE

- $f$ dimensionless streamfunction defined by equation (14)
- $G$ auxiliary velocity function, $\partial f/\partial\xi$
- $g$ acceleration due to gravity
- $Gr$ Grashof number, $[g\beta K(T_b-T_\infty)L]/\nu^2$
- $h$ local heat transfer coefficient
- $h^*$ dimensionless local heat transfer coefficient
- $H$ auxiliary velocity function, $\partial G/\partial\xi$
- $K$ permeability of the porous medium
- $k$ thermal conductivity of the porous medium
- $k_f$ conductivity of the fin
- $Ncc$ conjugate convection–conduction parameter defined by equation (4)
- $Pe$ Péclet number, $u_\infty L/\alpha$
- $Pr$ Prandtl number, $\nu/\alpha$
- $q$ local heat flux
- $r$ coordinate in the transverse direction
- $r_0$ radius of the cylindrical fin
- $Re$ Reynolds number, $u_\infty L/\nu$
- $T$ temperature
- $u$ Darcy's velocity component in the $x$-direction
- $v$ Darcy's velocity component in the $r$-direction
- $x$ coordinate in the axial direction.

Greek symbols

- $\alpha$ equivalent thermal diffusivity
- $\beta$ coefficient of thermal expansion
- $\eta$ pseudosimilarity variable defined by equation (14)
- $\eta_{eff}$ efficiency of the fin
- $\xi$ dimensionless variable in the $x$-direction
- $\theta$ dimensionless temperature of the fluid defined by equation (13)
- $\lambda$ surface curvature parameter defined by equation (19)
- $\mu$ viscosity of the convective fluid in the porous medium
- $\nu$ kinematic viscosity of the convective fluid
- $\rho$ density of the convective fluid
- $\phi$ auxiliary temperature function, $\partial\theta/\partial\xi$
- $\chi$ auxiliary temperature function, $\partial\phi/\partial\xi$
- $\psi$ streamfunction defined by equation (9)
- $\Omega$ buoyancy force parameter, $Gr/Re$.

Subscripts

- $\infty$ condition at infinity
- b condition at the fin base
- f variable associated with the fin.

force is acting in the same direction as the external flow.

If the radius of the fin $r_0$ is small compared with the length of the fin $L$, heat conduction within the fin can be considered to be one-dimensional. It follows that the governing equation for temperature distribution along the fin $T_f$ is

$$k_f r_0 \frac{d^2T_f}{dx^2} = h(x)(T_f - T_\infty) \tag{1}$$

where $k_f$ is the thermal conductivity of the fin and the $h(x)$ is the local heat transfer coefficient which is to be determined. The boundary conditions for the fin are

$$x = L: \quad T_f = T_b \tag{2}$$

$$x = 0: \quad \frac{dT_f}{dx} = 0 \tag{3}$$

where an adiabatic boundary condition at the tip of the fin is assumed. Equation (1) can be rewritten in the following dimensionless form:

$$\frac{d^2\theta_f}{d\xi^2} = (Ncc)\,h^*(\xi)\theta_f \tag{4}$$

where $\theta_f = (T_f - T_\infty)/(T_b - T_\infty)$ is the dimensionless temperature of the fin; $\xi = x/L$ is the dimensionless distance; $Ncc = (k/k_f)(2L/r_0)\sqrt{Re}$ is the conjugate convection–conduction parameter with $k$ denoting the thermal conductivity of the porous medium and $Re = u_\infty L/\nu$ denoting the Reynolds number; and $h^*(\xi) = hL/k\sqrt{Re}$ is the dimensionless local heat transfer coefficient which remains to be determined. Equations (2) and (3) in terms of the dimensionless temperature are

$$\xi = 1: \quad \theta_f = 1 \tag{5}$$

$$\xi = 0: \quad \frac{d\theta_f}{d\xi} = 0. \tag{6}$$

If the Boussinesq approximation and the boundary-layer approximation are invoked and the Darcy's law is applicable, the governing equations in a cylindrical coordinate for flow in the porous medium are [9]

$$\frac{\partial}{\partial r}\left(\frac{1}{r}\frac{\partial\psi}{\partial r}\right) = \frac{\rho_\infty g\beta K}{\mu}\frac{\partial T}{\partial r} \tag{7}$$

$$\alpha\frac{\partial}{\partial r}\left(r\frac{\partial T}{\partial r}\right) = \left(\frac{\partial\psi}{\partial r}\frac{\partial T}{\partial x} - \frac{\partial\psi}{\partial x}\frac{\partial T}{\partial r}\right) \tag{8}$$

where $\rho_\infty$, $\mu$ and $\beta$ are the density of the fluid at infinity, the viscosity and thermal expansion coefficient of the fluid, respectively; $K$ is the permeability of the porous medium; $\alpha$ is the equivalent thermal diffusivity of the saturated porous medium; $g$ is the gravitational acceleration; and $T$ is the temperature of the fluid which is in thermal equilibrium with the porous

medium. The streamfunction $\psi$ is defined as

$$u = \frac{1}{r}\frac{\partial \psi}{\partial r} \quad \text{and} \quad v = -\frac{1}{r}\frac{\partial \psi}{\partial x} \tag{9a, b}$$

where $u$ and $v$ are the Darcian velocities in the $x$- and $r$-directions, respectively.

Equations (7) and (8) are subject to the following boundary conditions:

$$r = r_0: \quad \frac{\partial \psi}{\partial x} = 0, \quad T = T(x, r_0) \tag{10a, b}$$

and

$$y \to \infty: \quad \frac{1}{r}\frac{\partial \psi}{\partial r} = u_\infty, \quad T = T_\infty \tag{11a, b}$$

where $T(x, r_0)$ is the temperature of the fluid along the impermeable surface of the fin.

As a first step toward solving equations (7)–(11), these equations are first transformed through an appropriate set of new variables to reduce the axial dependence of the solution. For this purpose, the following transformations are introduced:

$$\psi = r_0(\alpha u_\infty x)^{1/2} f(\eta, \xi) \tag{12}$$

$$\theta(\eta, \xi) = \frac{T - T_\infty}{T_b - T_\infty} \tag{13}$$

$$\eta = \frac{r^2 - r_0^2}{2r_0}\left(\frac{u_\infty}{x\alpha}\right)^{1/2} \tag{14}$$

where $\xi$ is defined in equation (4). Substituting equations (12)–(14) into (9a, b) yields

$$u = u_\infty \frac{\partial f}{\partial \eta}(\eta, \xi) \tag{15}$$

$$v = -\frac{r_0}{2r}\left(\frac{\alpha u_\infty}{x}\right)^{1/2}\left(\eta\frac{\partial f}{\partial \eta} + 2\xi\frac{\partial f}{\partial \xi} + f\right). \tag{16}$$

When the transformations given by equations (12)–(14) are applied to (7) and (8), there results

$$\frac{\partial^2 f}{\partial \eta^2} = \Omega\frac{\partial \theta}{\partial \eta} \tag{17}$$

$$(1 + \lambda\sqrt{\xi}\eta)\frac{\partial^2 \theta}{\partial \eta^2} + \left(\frac{1}{2}f + \lambda\sqrt{\xi}\right)\frac{\partial \theta}{\partial \eta} = \xi\left(\frac{\partial f}{\partial \eta}\frac{\partial \theta}{\partial \xi} - \frac{\partial \theta}{\partial \eta}\frac{\partial f}{\partial \xi}\right) \tag{18}$$

where

$$\Omega = \frac{g\beta K(T_b - T_\infty)L/\nu^2}{u_\infty L/\nu} = Gr/Re$$

is the mixed convection parameter which is a measure of the relative importance of the free to forced convection. The quantity $\lambda$ in equation (18) is defined as

$$\lambda = \frac{2L}{r_0}\sqrt{\frac{\alpha}{u_\infty L}} \tag{19}$$

which is a measure of the surface curvature of the vertical cylinder. It is relevant to note that $\lambda = 0$ reduces to that of a plate fin [6]. Equations (10) and (11) after the transformation become

$$\xi\frac{\partial f}{\partial \xi}(0, \xi) + \tfrac{1}{2}f(0, \xi) = 0, \quad \theta = (0, \xi) \tag{20a, b}$$

$$f'(\infty, \xi) = 1, \quad \theta(\infty, \xi) = 0. \tag{21a, b}$$

Equations (17)–(21) are coupled with (4)–(6) through the following interface conditions

$$r = r_0: \quad T(x, 0) = T_f(x) \tag{22}$$

$$r = r_0: \quad -k\frac{\partial T}{\partial r} = h(x)(T_f - T_\infty) \tag{23}$$

where equation (22) requires that temperature is continuous while equation (23) requires that heat flux is continuous across the fin–fluid interface. Equations (22) and (23) in terms of the new variables defined in (12)–(14) are

$$\theta_f(\xi) = \theta(0, \xi) \tag{24}$$

$$h^*(\xi) = \sqrt{Pr}\,\frac{[-\theta'(0, \xi)]}{\sqrt{\xi}\theta_f(\xi)} \tag{25}$$

where $Pr = \nu/\alpha$ is the Prandtl number. Equations (4)–(6) and (17)–(21) with (24) and (25) constitute the governing equations and boundary conditions for the present problem.

*Local nonsimilarity solution*

Equations (17)–(21) show that the boundary-layer flow in the porous medium does not admit a similarity solution. The nonsimilarities arise from the surface curvature of the cylindrical fin, the buoyancy force term and the nonuniform temperature distribution of the fin.

Equations (17)–(21) will now be approximated by a set of ordinary differential equations by the local nonsimilarity method [7, 8]. Following the standard procedure [7, 8], one can derive an approximate set of ordinary differential equations for each 'level of truncation', which is designated for the elimination of terms involving $\xi$-derivatives in the governing equations at different stages of development.

For the first level of truncation, the terms involving $\partial f/\partial \xi$ or $\partial \theta/\partial \xi$ are deleted in equations (18) and (20a) which lead to

$$f'' = \Omega\theta' \tag{26}$$

$$(1 + \lambda\sqrt{\xi}\eta)\theta'' + (\tfrac{1}{2}f + \lambda\sqrt{\xi})\theta' = 0 \tag{27}$$

$$f(0, \xi) = 0, \quad \theta(0, \xi) = \theta_f(\xi) \tag{28a, b}$$

$$f'(\infty, \xi) = 1, \quad \theta(\infty, \xi) = 0 \tag{29a, b}$$

where the primes are the derivatives with respect to $\eta$. It is pertinent to note that $\xi$ plays the role of a parameter in equations (26)–(29).

For the second level of truncation, new functions $G = \partial f/\partial \xi$ and $\phi = \partial \theta/\partial \xi$ are introduced in equations (18) and (20a). With this insertion, all terms in (18) and (20a) are retained without approximation. Additional

equations and boundary conditions for the new unknowns $G$ and $\phi$ are generated by taking derivatives of (17)–(21) with respect to $\xi$ and discarding the terms containing $\partial G/\partial\xi$ and $\partial\phi/\partial\xi$. This leads to the following equations and boundary conditions for the second level of truncation:

$$f''' = \Omega\theta' \tag{30}$$

$$(1+\lambda\sqrt{\xi}\eta)\theta'' + (\tfrac{1}{2}f + \lambda\sqrt{\xi})\theta' = \xi(f'\phi - \theta' G) \tag{31}$$

$$G'' = \Omega\phi' \tag{32}$$

$$(1+\lambda\sqrt{\xi}\eta)\phi'' + (\tfrac{1}{2}f + \lambda\sqrt{\xi} + \xi G)\phi' = (f' + \xi G')\phi - \frac{\lambda\eta}{2\sqrt{\xi}}\theta'' - \left(\frac{3}{2}G + \frac{\lambda}{2\sqrt{\xi}}\right)\theta' \tag{33}$$

with

$$f(0,\xi) = 0, \quad G(0,\xi) = 0 \tag{34a, b}$$

$$\theta(0,\xi) = \theta_f(\xi), \quad \phi(0,\xi) = \frac{d\theta_f}{d\xi}(\xi) \tag{35a, b}$$

$$f'(\infty,\xi) = 1, \quad G'(\infty,\xi) = 0 \tag{36a, b}$$

$$\theta(\infty,\xi) = 0, \quad \phi(\infty,\xi) = 0. \tag{37a, b}$$

Similarly, the equations and boundary conditions for the third level of truncation are

$$f''' = \Omega\theta' \tag{38}$$

$$(1+\lambda\sqrt{\xi}\eta)\theta'' + (\tfrac{1}{2}f + \lambda\sqrt{\xi})\theta' = \xi(f'\phi - \theta' G) \tag{39}$$

$$G'' = \Omega\phi' \tag{40}$$

$$(1+\lambda\sqrt{\xi}\eta)\phi'' + (\tfrac{1}{2}f + \lambda\sqrt{\xi} + \xi G)\phi' = (f' + \xi G')\phi - \frac{\lambda\eta}{2\sqrt{\xi}}\theta'' - \left(\frac{3}{2}G + \frac{\lambda}{2\sqrt{\xi}} + \xi H\right)\theta' + \xi f'\chi - \xi H\theta' \tag{41}$$

$$H'' = \Omega\chi' \tag{42}$$

$$(1+\lambda\sqrt{\xi}\eta)\chi'' + (\tfrac{1}{2}f + \lambda\sqrt{\xi} + \xi G)\chi' = 2(f' + \xi G')\chi - \frac{\lambda\eta}{\sqrt{\xi}}\phi'' - \left(3G + \frac{\lambda}{\sqrt{\xi}} + 2\xi H\right)\phi' + (2G' + \xi H')\phi + \frac{\lambda\eta}{4\sqrt{\xi^3}}\theta'' - \left(\frac{5}{2}H - \frac{\lambda}{4\sqrt{\xi^3}}\right)\theta' \tag{43}$$

with

$$f(0,\xi) = 0, \quad G(0,\xi) = 0, \quad H(0,\xi) = 0 \tag{44a, b, c}$$

$$\theta(0,\xi) = \theta_f(\xi), \quad \phi(0,\xi) = \frac{d\theta_f}{d\xi}(\xi), \quad \chi(0,\xi) = \frac{d^2\theta_f}{d\xi^2}(\xi) \tag{45a, b, c}$$

$$f'(\infty,\xi) = 1, \quad G'(\infty,\xi) = 0, \quad H'(\infty,\xi) = 0 \tag{46a, b, c}$$

$$\theta(\infty,\xi) = 0, \quad \phi(\infty,\xi) = 0, \quad \chi(\infty,\xi) = 0 \tag{47a, b, c}$$

where $H = \partial G/\partial\xi$ and $\chi = \partial\phi/\partial\xi$.

## RESULTS AND DISCUSSION

Both the heat conduction equation for the fin and the local nonsimilarity equations for the convective flow in the porous medium are second-order ordinary differential equations with two-point boundary conditions. These coupled equations can be converted into an integral form and numerical solutions can be obtained by iteration. The details of the procedure are described in ref. [6] and will not be repeated here. Computations were carried out up to the third level of truncation with selected values of $\lambda$, $\Omega$, $Ncc$ and at a Prandtl number of 5.5. The following are the results based on the third level of truncation.

*Fin temperature distributions*

Figures 2 and 3 present fin temperature distributions for $\lambda = 2.0$ and 5.0 and for representative values of $Ncc$ and $\Omega$. It is observed that the fin temperatures increase monotonically from the tip ($\xi = 0.0$) to the base ($\xi = 1.0$) for all cases. Also, it is seen that larger values of $Ncc$ give rise to larger fin temperature variations. This behavior is evident from the definition of $Ncc$ which shows that higher values of $Ncc$ correspond to low fin conductances and high convection effects, thus resulting in increased temperature variations. In addition, higher values of $\Omega$ amplify these variations due to the fact that buoyancy force enhances the heat transfer rates. The figures also show that higher values of $\lambda$ also give rise to more significant fin temperature variations.

*Local heat transfer coefficients*

The local heat transfer coefficient is defined as

$$h(x) = \frac{-k\left.\dfrac{\partial T}{\partial r}\right|_{r=r_0}}{T_f - T_\infty} \tag{48}$$

which in a dimensionless form becomes

$$\frac{hL}{k\sqrt{Re}} = \sqrt{Pr}\,\frac{[-\theta'(\xi,0)]}{\sqrt{\xi}\,\theta_f(\xi)}. \tag{49}$$

Representative distributions for $\lambda = 2.0$ and 5.0, and selected values of $Ncc$ and $\Omega$ are presented in Figs. 4 and 5. The figures show that when $\Omega = 0.0$ (pure forced convection), the heat transfer coefficients decrease monotonically from large values near the tip to some finite values at the root for all values of $Ncc$ and $\lambda$. For a mixed convection flow ($\Omega \neq 0.0$) an increase of $Ncc$, representing an increase of fin temperature variations, gives rise to an enhanced buoyancy force along the streamwise direction. Therefore, at a high value of $Ncc$ ($Ncc = 1.5$, for example) the local heat transfer coefficients decrease at first, attain a minimum value, and then increase with increasing streamwise direction. It is also observed that as $Ncc$ increases, the location of the minimum shifts toward the tip, and the extent of the downstream rise becomes greater. Also, for given values of $Ncc$ and $\Omega$, higher local heat transfer coefficients are seen at higher values of $\lambda$.

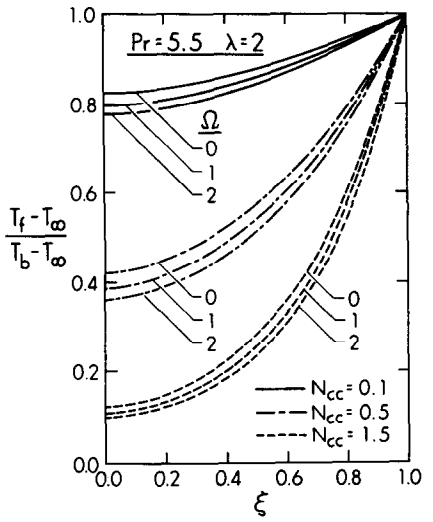


FIG. 2. Fin temperature distributions for $\lambda = 2$.

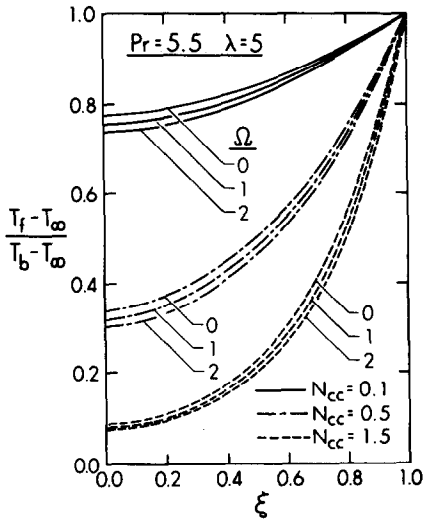


FIG. 3. Fin temperature distributions for $\lambda = 5$.

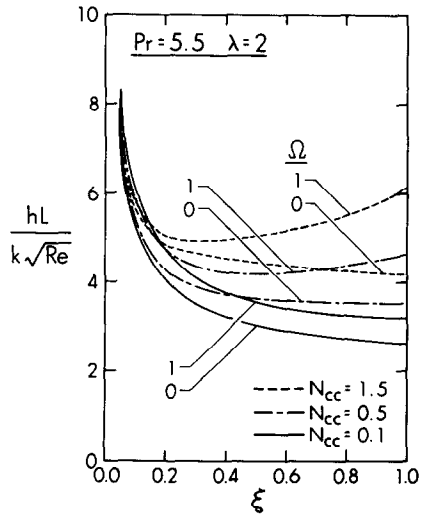


FIG. 4. Local heat transfer coefficients for $\lambda = 2$.

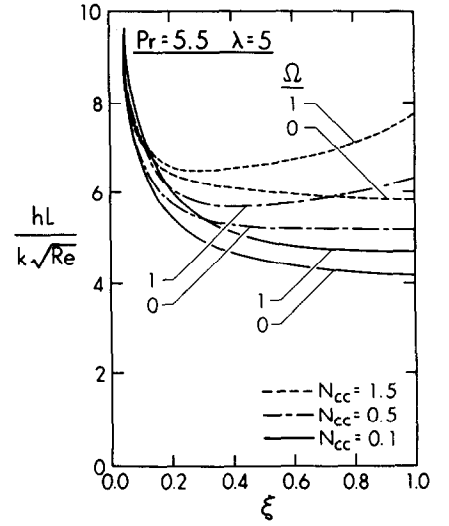


FIG. 5. Local heat transfer coefficients for $\lambda = 5$.

*Local heat fluxes*

The local heat flux can be expressed as

$$q = -k \left.\frac{\partial T}{\partial r}\right|_{r=r_0} \tag{50}$$

which can be cast in dimensionless form as

$$\frac{qL}{k(T_b - T_\infty)\sqrt{Re}} = \sqrt{Pr}\,\frac{[-\theta'(0,\xi)]}{\sqrt{\xi}}. \tag{51}$$

The results of dimensionless local heat fluxes are given in Figs. 6 and 7. It can be seen that for a given $\lambda$, the buoyancy force increases the local heat flux. Also, as the value of *Ncc* is increased, most of the heat transfer to the fluid takes place in the neighborhood of the fin root. This is due to the fact that a larger *Ncc*, representing a lower thermal conductivity of the fin, results in a higher temperature near the root.

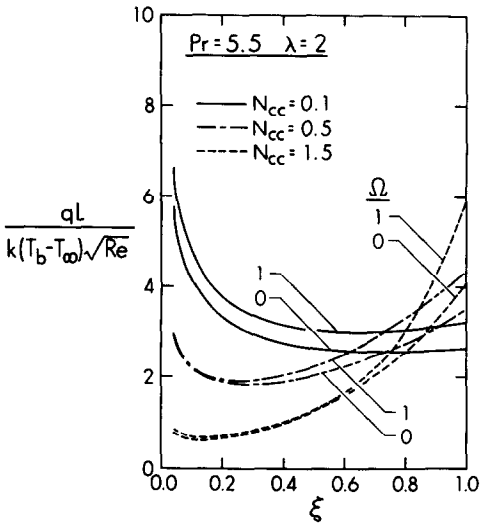


FIG. 6. Local heat fluxes for $\lambda = 2$.

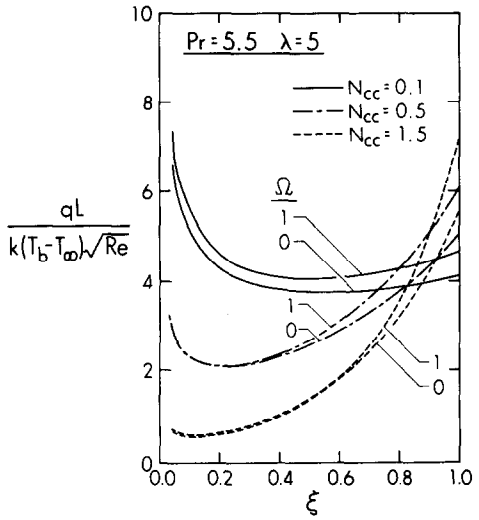


FIG. 7. Local heat fluxes for $\lambda = 5$.

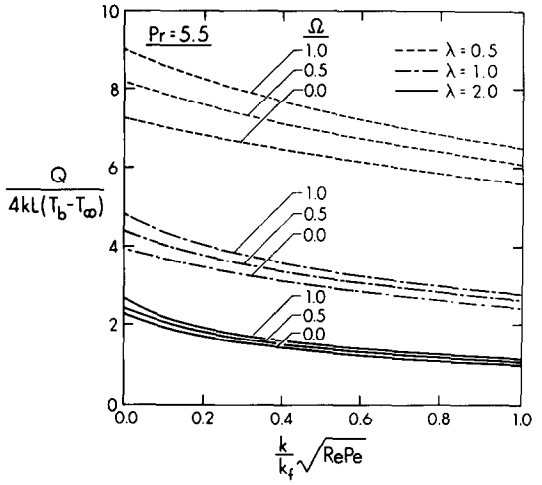


FIG. 8. Total heat transfer rates.

If the results in Fig. 6 are compared with those in Fig. 7, one can see that the local heat flux is higher for a higher value of $\lambda$. However, one should note that the radius of a fin could be different for each $\lambda$. Thus, lower values of the local heat flux for low $\lambda$s do not necessarily imply that the total heat flux over the fin surface is lower than that for larger $\lambda$s. This will be discussed further below.

*Total heat transfer rate*

The total heat transfer rate can be obtained from

$$Q = 2\pi r_0 \int_0^L q(x)\,\mathrm{d}x = -2\pi r_0 k \int_0^L \left(\frac{\partial T}{\partial r}\right)_{r=r_0} \mathrm{d}x \quad (52)$$

which can be rewritten in dimensionless form as

$$\frac{Q}{\pi r_0 k(T_b - T_\infty)\sqrt{Re}} = -2\sqrt{Pr}\,F(\Omega, \lambda, Ncc) \quad (53)$$

where

$$F(\Omega, \lambda, Ncc) = \int_0^1 \frac{\theta'(0, \xi)}{\sqrt{\xi}}\,\mathrm{d}\xi. \quad (54)$$

In the above expressions, both the LHS of equation (53) and the parameter $Ncc$ contain $r_0$. Thus, the effect of curvature on the total heat transfer rate cannot be observed directly from equation (53). To get rid of the $r_0$-dependence, both the LHS of equation (53) and $Ncc$ are divided by $\lambda$ to give

$$\frac{Q}{4kL(T_b - T_\infty)} = -\pi F[\Omega, \lambda, (Pe\,Re)^{1/2}k/k_f] \quad (55)$$

where $Ncc/\lambda = (Pe\,Re)^{1/2}k/k_f$ with $Pe = u_\infty L/\alpha$ denoting the Péclet number. Equation (55) is plotted as $Q/4kL(T_b - T_\infty)$ vs $(Pe\,Re)^{1/2}k/k_f$ at selected values of $\lambda$ and $\Omega$ in Fig. 8. It is shown that smaller values of $\lambda$ gives rise to higher value of the total heat transfer rate. This is expected, as a smaller value of $\lambda$ represents a larger value of $r_0$ (i.e. a larger convection surface), and therefore results in a larger value of the total heat transfer rate.

*Fin efficiency*

The fin efficiency is defined as

$$\eta_{eff} = Q/Q_{iso} \quad (56)$$

where $Q_{iso}$ denotes the total heat transfer rate resulting from an isothermal fin. The results of $\eta_{eff}$ vs $(Pe\,Re)^{1/2}k/k_f$ are presented in Fig. 9 for representative values of $\lambda$ and $\Omega$. These results indicate that a high value of $\lambda$ (representing a smaller radius) gives rise to a smaller fin efficiency as expected. Also, the efficiency decreases as $\Omega$ or $(Re\,Pe)^{1/2}k/k_f$ is increased.

## CONCLUDING REMARKS

The present analysis has yielded the solution of conjugate, mixed convection–conduction heat transfer

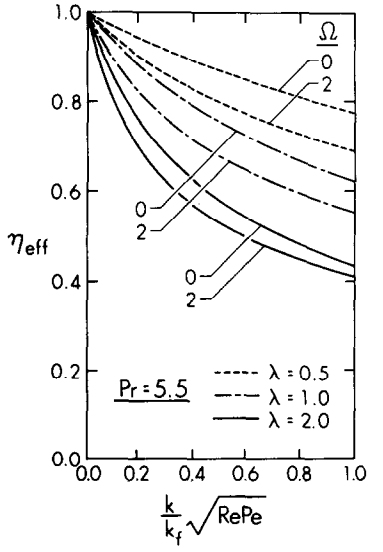


FIG. 9. Fin efficiencies.

about a vertical, cylindrical fin embedded in a porous medium. The trends of the results obtained in this paper are similar to those of plate fin solutions obtained in a previous study [6]. It should be noted that the plate fin solution may be obtained from the present analysis simply by letting $\lambda = 0$, which implies an infinite radius, or equivalently a flat plate.

## REFERENCES


1. E. M. Sparrow and S. Acharya, A natural convection fin with a solution-determined nonmonotonically varying heat transfer coefficient, *J. Heat Transfer* **103,** 218–225 (1981).
2. E. M. Sparrow and M. K. Chyu, Conjugate forced convection–conduction analysis of heat transfer in a plate fin, *J. Heat Transfer* **104,** 204–206 (1982).
3. B. Sunden, Conjugate mixed convection heat transfer from a vertical rectangular fin, *Int. Comm. Heat Mass Transfer* **10,** 267–276 (1983).
4. M. J. Huang, C. K. Chen and J. W. Cleaver, Vertical circular pin with conjugated natural convection–conduction flow, *J. Heat Transfer* **107,** 242–245 (1985).
5. M. J. Huang and C. K. Chen, Conjugate mixed convection and conduction heat transfer along a vertical circular pin, *Int. J. Heat Mass Transfer* **28,** 523–529 (1985).
6. J. Y. Liu, W. J. Minkowycz and P. Cheng, Conjugate mixed convection heat transfer analysis of a plate fin embedded in a porous medium, *Numer. Heat Transfer* **9,** 453–468 (1986).
7. W. J. Minkowycz and E. M. Sparrow, Numerical solution scheme for local nonsimilarity boundary layer analysis, *Numer. Heat Transfer* **1,** 69–85 (1978).
8. W. J. Minkowycz and E. M. Sparrow, Interaction between surface mass transfer and transverse curvature in natural convection boundary layers, *Int. J. Heat Mass Transfer* **22,** 1445–1454 (1979).
9. W. J. Minkowycz and P. Cheng, Free convection about a vertical cylinder embedded in a porous medium, *Int. J. Heat Mass Transfer* **19,** 805–813 (1976).


## CONDUCTION THERMIQUE COUPLEE A LA CONVECTION MIXTE, LE LONG D'UNE AILETTE CYLINDRIQUE DANS UN MILIEU POREUX


**Résumé**—On étudie analytiquement le problème de la convection mixte autour d'une ailette verticale, cylindrique, noyée dans un milieu poreux, à partir de la théorie du couplage convection–conduction. Une solution locale non affine, jusqu'au troisième niveau de troncature, est obtenue pour la convection dans le milieu poreux. Le système d'équations différentielles est couplé à l'équation monodimensionnelle de conduction dans l'ailette à travers les conditions à l'interface. On illustre les effets du paramètre de couplage convection–conduction, de la courbure de la surface et du paramètre de convection mixte, sur la distribution de température, sur le coefficient de transfert local, sur le flux local, le transfert thermique global et sur l'efficacité de l'ailette. Les résultats de la présente étude ont des allures semblables à ceux relatifs aux fluides classiques.


## WÄRMEÜBERTRAGUNG DURCH MISCH-KONVEKTION UND WÄRMELEITUNG ENTLANG EINER ZYLINDRISCHEN RIPPE IN EINEM PORÖSEN MEDIUM


**Zusammenfassung**—Die Misch-Konvektion an einer vertikalen, zylindrischen Rippe in einem porösen Medium wird analytisch mit Hilfe der Theorie der gekoppelten Wärmeübertragung durch Konvektion und Leitung untersucht. Für die Konvektionsströmung im porösen Medium wird eine örtliche nichtähnliche Lösung ermittelt. Der gewonnene Satz gewöhnlicher Differentialgleichungen wird mit der Gleichung für die eindimensionale Wärmeleitung in der Rippe über Schnittstellenbedingungen gekoppelt. Die Einflüsse der Parameter der gekoppelten Wärmeübertragung, der Oberfächenform und der Misch-Konvektion auf die Temperaturverteilung in der Rippe, den örtlichen und den gesamten Wärmeübergangskoeffizienten, die örtliche Wärmestromdichte sowie auf den Rippenwirkungsgrad werden dargestellt. Die Ergebnisse dieser Untersuchung zeigen Abhängigkeiten ähnlich wie bei klassischen Fluiden.


## СОПРЯЖЕННЫЙ ТЕПЛОПЕРЕНОС СМЕШАННОЙ КОНВЕКЦИЕЙ И ПРОВОДИМОСТЬЮ ОКОЛО ЦИЛИНДРИЧЕСКОГО РЕБРА В ПОРИСТОЙ СРЕДЕ


**Аннотация**—На основе сопряженной постановки конвективно-кондуктивного теплообмена аналитически изучается задача смешанноконвективного течения у вертикального цилиндрического ребра, погруженного в пористую среду. Для конвективного течения в пористой среде получено локальное неавтомодельное решение. Выведенная в результате система обыкновенных дифференциальных уравнений объединяется с уравнением одномерного теплопереноса в ребре через граничные условия. Показано влияние сопряженного конвективно-кондуктивного параметра, кривизны поверхности и коэффициента смешанной конвекции на распределение температуры ребра, локальный коэффициент теплопереноса, локальный теплообмен, общий теплоперенос и эффективность ребра. Результаты аналогичны данным для жидкостей.